Available online at www.sciencedirect.com
ScienceDirect
Trans. Nonferrous Met. Soc. China 28(2018) 1275−1286
Transactions of Nonferrous Metals Society of China
www.tnmsc.cn

Quality index and hot tearing susceptibility of Al−7Si−0.35Mg−*x*Cu alloys

R. TAGHIABADI[1], A. FAYEGH[1], A. PAKBIN[1], M. NAZARI[1], M. H. GHONCHEH[2]

1. Department of Materials Science and Ceramic Engineering, Imam Khomeini International University, Qazvin, Iran;
2. School of Metallurgy and Materials Engineering, Iran University of Science and Technology, Tehran, Iran

Received 25 June 2017; accepted 28 December 2017

Abstract: The effects of Cu addition (0.5%, 1%, 1.5%, 2%, and 3%, mass fraction) on the quality index (Q_i) and hot tearing susceptibility (HTS) of A356 alloy were investigated. According to the results, Cu addition up to 1.5% increases the Q_i by almost 10%, which seems to be due to its solid solution strengthening and dispersion hardening effect of Cu-rich Al_2Cu and AlMgCuSi compounds. However, further addition of Cu (up to 3%) decreases the Q_i by almost 12%, which is likely due to the reduction of tensile strength and elongation caused by increased volume fraction of brittle Cu-rich intermetallics and microporosities in the microstructure. It is also found that Cu increases the HTS of A356 alloy measured by constrained rod casting method. According to the thermal analysis results, Cu widens the solidification range of the alloy, which in turn, decreases its fluidity and increases the time period during which the mushy-state alloy is exposed to the hot tearing susceptible zone. SEM examination of the hot tear surfaces in high-Cu alloys also demonstrates their rough nature and the occurrence of interdendritic/intergranular microcracks as convincing evidences for the initiation of hot tears in the late stages of solidification in which there is not enough time for crack healing.
Key words: Al−Si−Mg alloy; hot tearing; quality index; copper; fluidity

1 Introduction

A356 alloy (Al−7Si−0.35Mg) shows great potential for several engineering applications. The growing tendency towards the use of this alloy is directly related to its specific advantages, including low density, excellent fluidity, good tribological properties, high thermal conductivity, and very good corrosion resistance [1,2]. This alloy also has very high specific strength in heat-treated condition which is attributed to the formation of fine coherent Mg_2Si particles in its matrix [2−4]. Moreover, significant amounts of Si in the composition of A356 alloy makes it less prone to the casting defects like shrinkage porosities and hot tears as compared to other important alloys like Al−Cu, Al−Mg, and Al−Zn−Mg alloys [5,6].

Copper is one of the most common alloying elements for A356 alloy mainly due to its strengthening effect. Research has shown that Cu in combination with Mg promotes the formation of θ-Al_2Cu precipitates, thereby enhances the aging characteristics of the alloy [4,7,8]. In addition to the increased room-temperature strength, Cu addition also improves the high-temperature strength of A356 alloy and decreases its coefficient of thermal expansion [4,9,10]. Nevertheless, it has been reported that Cu significantly increases the amount of microporosities in the microstructure of Al−Si−Mg alloys and exerts negative impact on their casting fluidity and feeding characteristics [11,12].

Hot tearing is one of the most serious casting defects which substantially decreases the productivity of a casthouse. Many attempts have been made to understand this phenomenon and the mechanisms involved. According to the findings, hot tears are formed by the cooperation of two complementary phenomena: insufficient feeding of the liquid metal in a vulnerable temperature range, and local tensile strain build-up in the solidified part of the casting, which are principally arisen from the constraint of alloy thermal contraction and/or density change when the alloy transforms from liquid to solid [13−16].

Feeding characteristic of the alloys is substantially influenced by their chemistry. In this regard, extensive work has been carried out and still is being conducted to investigate the effect of chemical composition (and impurities) on the hot tearing response of Al alloys. The

Corresponding author: R. TAGHIABADI; Tel/Fax: +98-28-33901156; E-mail: taghiabadi@ikiu.ac.ir
DOI: 10.1016/S1003-6326(18)64783-1

effect of various additive elements on the hot tearing response of Al−4.5Cu and Al−4.5Cu−5Si alloys was investigated by OYA et al [17]. It was shown that the addition of Ti, Mg, and Si has a positive impact on the hot tearing resistance, but Sn, Zn, Fe, and Ni impair it. LI et al [18] investigated the effect of Y on the hot tearing resistance of Al−5Cu alloy. It was found that the addition of Y decreases the amount of grain boundary liquid, reduces the temperature at which α(Al) phase begins to solidify, narrows the freezing range of the alloy, and increases its hot tearing resistance. NAGAUMI et al [19] found that Fe impurity has an adverse effect on the hot tearing resistance of Al−Mg−Si alloys. This behavior was attributed to the formation of Fe-rich α-AlFeMn compounds.

The influence of Mn and Cu addition on the hot tearing response of Al−Mg−Si alloys was also investigated. It was found that the hot tearing was insensitive to Cu content, and highly sensitive to Mn content [20].

Most of the studies have focused on Al−Cu and Al−Mg alloys because of their high susceptibility to the hot tearing, but very limited efforts have been made so far to study the hot tearing of Al−Si-based alloys. This is probably because these alloys have significant fluidity and considerable feeding characteristic due to the presence of Si. However, previous studies have shown that the Cu addition has a negative effect on the fluidity of Al−Si alloys and significantly increases the shrinkage porosity in their structure. Therefore, the aim of the present study is to investigate the concurrent effect of Cu, as an important alloying addition, on the quality index and hot tearing susceptibility of widely used A356 Al−Si alloy.

2 Experimental

Based on the main chemical composition of A356 alloy, the code and the chemical composition of experimental alloys used in the present study are shown in Table 1. The alloys were prepared by melting in a clay-graphite crucible using an electrical resistance furnace. Desired amount of Cu was added to the liquid alloy using pure copper (99.9%).

Table 1 Alloy code and chemical composition of experimental alloys (mass fraction, %)

Alloy code	Si	Mg	Cu	Fe	Ni	Cr	Mn	Zn	Al
Base	7.18	0.39	0.01	<0.1	0.01	0.01	0.32	0.24	Bal.
C0.5	7.20	0.37	0.48	<0.1	0.01	0.01	0.32	0.22	Bal.
C1	7.07	0.36	0.94	<0.1	0.01	0.01	0.30	0.25	Bal.
C1.5	7.09	0.34	1.54	<0.1	0.01	0.01	0.31	0.22	Bal.
C2	7.08	0.36	2.18	<0.1	0.01	0.01	0.29	0.23	Bal.
C3	7.12	0.35	3.04	<0.1	0.01	0.01	0.30	0.24	Bal.

After degassing with C_2Cl_6-based tablets, the melt was superheated up to (100±5) °C above the liquidus temperature, stirred gently, and some of it was poured into a cast-iron constrained-rod casting (CRC) mold developed by Alcan Kingston Research and Development Center (AKRDC) (Fig. 1(a)) and the rest of it was poured into another cast-iron tensile specimen mold (ASTM B 557M−02a) (Figs. 1(b) and (c)). To minimize the effect of friction between the mold wall

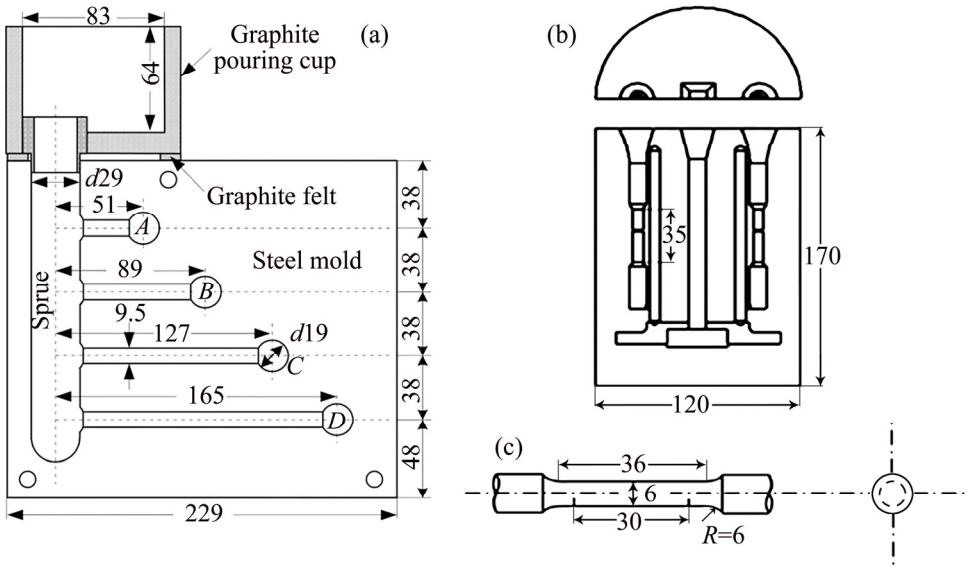

Fig. 1 Schematic diagram of constrained-rod casting (CRC) mold (a), tensile specimens mold (b), and dimensions and geometry of tensile specimens (c) (unit: mm)

and the solidifying melt, the mold cavity was preheated up to 250 °C, cleaned, and covered with graphite before each test.

The overall hot tear rating was calculated as the summation of individual hot tear rating of the four rods of CRC mold:

$$\mathrm{HTS}=\sum_{i=\mathrm{A}}^{\mathrm{D}}(C_i\times L_i) \quad (1)$$

where HTS is the overall hot tearing susceptibility of the alloys, L_i is length rating of the rod, where the hot tear occurs (Table 2), and C_i is the severity rating of each hot tear (Table 2)

Table 2 HTS rating system [13]

Rod type	Length/ mm	Numerical value, L_i	Hot tear severity	Numerical value, C_i
A	51	4	Complete separation	4
B	89	3	Severe	3
C	127	2	Light	2
D	165	1	Hair line	1

In the absence of hot tears, the C_i value is zero

By manipulating the HTS index, a second index in the form of a footprint chart was developed. Each axis in the footprint chart represents one rod and its value is the multiplication of C_i and L_i. The hot tearing susceptibility of the alloy is represented by area of the chart [13,21]. Footprint chart can easily show if hot tearing has taken place on a particular rod. The severity of the tear is also evident. The average of four measurements was reported as the final HTS value.

The alloy fluidity was measured by the vacuum suction method (Fig. 2). The molten alloy with desired temperature, held isothermally for desired time after skimming and stirring, was sucked into the silica glass tube under a predetermined pressure of 26664.4 Pa. After the completion of the solidification process, the flow length of the alloy samples was measured as fluidity length. The average of three measurements was reported as the final fluidity length.

A K-type thermocouple, inserted into a spherical cavity, was located at the end of 165 mm constrained rod (D-rod) and connected to a high-speed data acquisition system. The thermocouple was calibrated with melting and solidifying high purity Al (99.99%). Analog to digital (A/D) convertor used in this work had a sensitive 16-bit convertor (resolution of $1/2^{16}$ or 0.0015%), response time of 0.02 s and high accuracy detection. Time−temperature data were recorded with the frequency of 10 readings per second and it was plotted using Origin Pro.9.2 software (Origin Lab Corporation, Northampton, MA). In addition, solid fraction versus time was measured based on the Newtonian method.

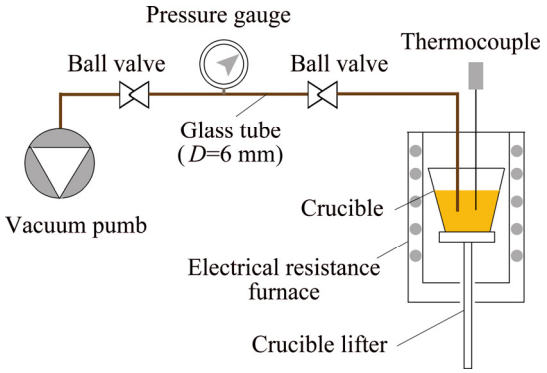

Fig. 2 Sketch of apparatus used for fluidity measurement

The tensile specimens were tensioned by a Zwick/Roell Z100 tensile testing machine at a constant crosshead speed of 0.5 mm/min. The average of four results was reported as the final value. Samples for metallographic observations were prepared by standard metallographic procedures and each cross-section was etched using 1% or 10% HF-distilled water reagent at room temperature for micro- or macro-structural characterization, respectively.

The effective grain size d_{eff} was evaluated by

$$d_{\mathrm{eff}}=f_{\mathrm{col}}\cdot d_{\mathrm{col}}+f_{\mathrm{eq}}\cdot d_{\mathrm{eq}} \quad (2)$$

where f_{col} and f_{eq} are the area fractions of columnar and equiaxed grains, and d_{col} and d_{eq} are the effective grain sizes of columnar (=0.5(length + radial diameter)) and equiaxed grains, respectively [22]. The grain size was measured via Carl Zeiss Axioskop-2-MAT microscope using the linear intercept method based on ASTM E112-12. The microstructures and tear morphologies were examined by a Tescan-Vega scanning electron microscope equipped with energy dispersive X-ray spectroscopy (EDS). In addition, the volume fraction of porosity (f) was measured by the following equation:

$$f=\frac{D_{\mathrm{t}}-D_{\mathrm{a}}}{D_{\mathrm{t}}}\times 100 \quad (3)$$

where D_{t} and D_{a} are the theoretical and actual densities of the alloy.

3 Results and discussion

3.1 Effect of Cu on microstructural characteristics and quality index

Figure 3 illustrates the SEM images of the base, C1, C2, and C3 alloys. According to the X-ray diffraction analysis (Fig. 4), the base alloy mainly consists of α(Al) matrix, the eutectic Si particles ($\mathrm{Si_E}$), and the $\mathrm{Mg_2Si}$

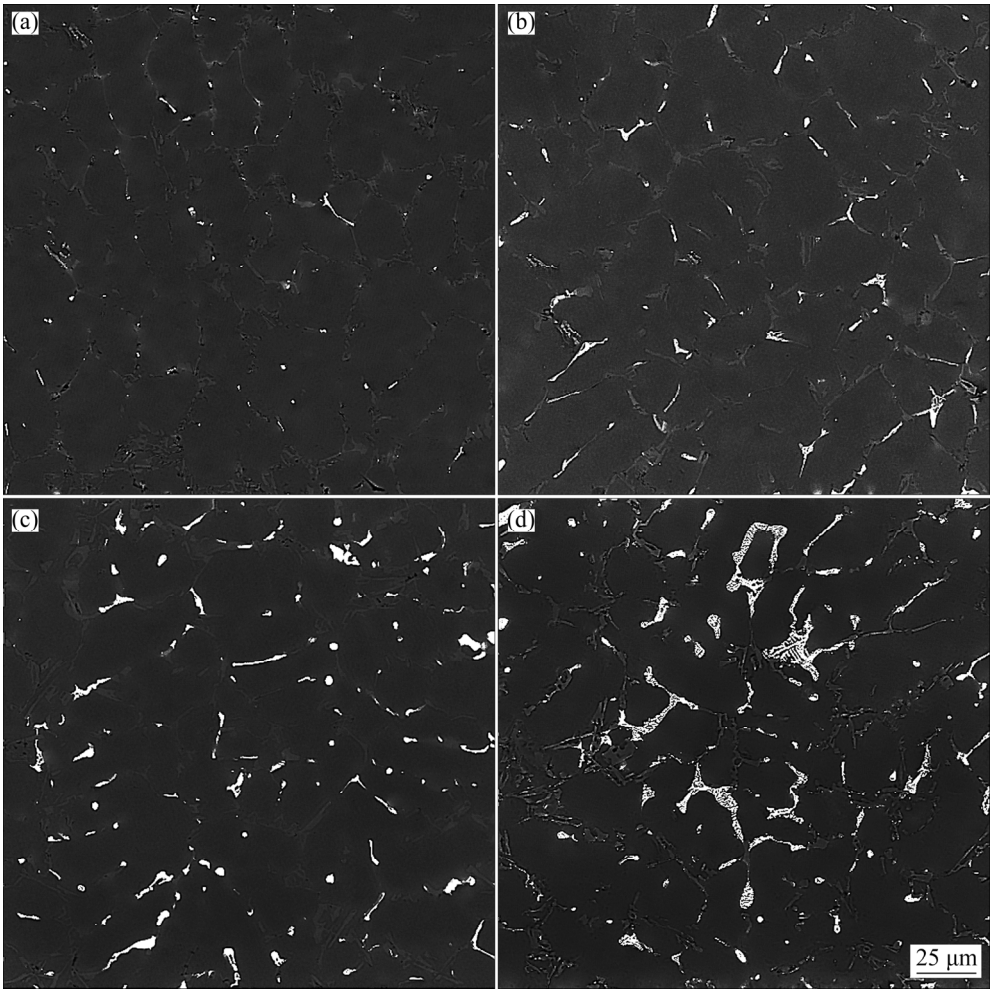

Fig. 3 SEM images of base (a), C1 (b), C2 (c), and C3 (d) alloys

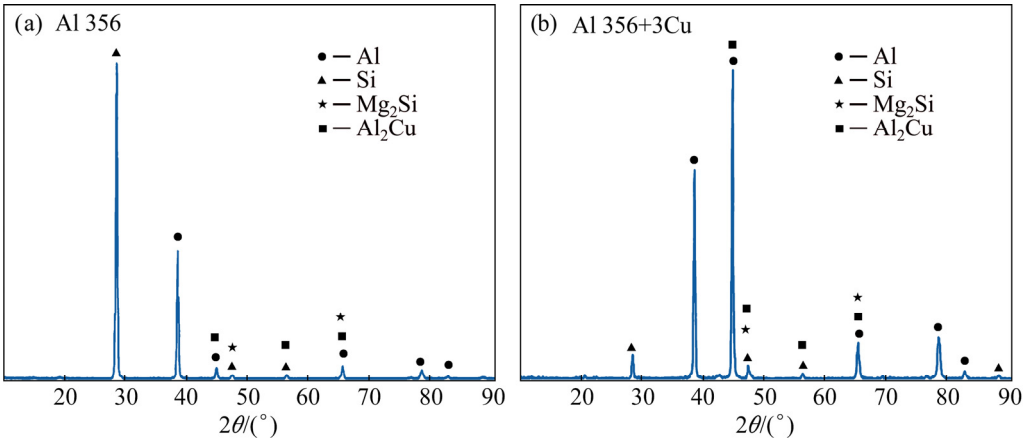

Fig. 4 XRD patterns of base (a) and C3 (b) alloy

particles. It is also evident from Figs. 3(b−d) that the addition of Cu leads to the formation of white precipitates in the matrix whose average size and volume fraction increase by its concentration. These particles, identified as θ-Al_2Cu (Fig. 4(b)), crystallized in two distinct forms which are namely blocky form and ternary eutectic $Al−Al_2Cu−Si_E$ pocket. The EDS analysis also reveals the presence of another AlMgCuSi phase in the microstructure (Fig. 5). Although, this quaternary particle is not detected by XRD probably due to its limited amounts.

The effect of Cu addition on the grain structure of A356 alloys is shown in Fig. 6. As seen, Cu addition turns the mixed columnar-equiaxed grain structures of

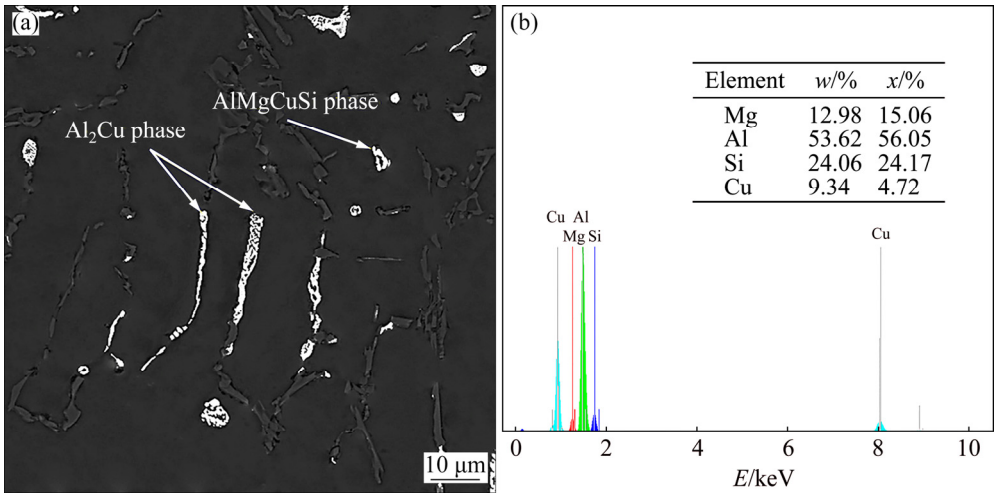

Fig. 5 SEM micrograph of C3 alloy (a) and EDS analysis of AlMgCuSi phase (b) shown in (a)

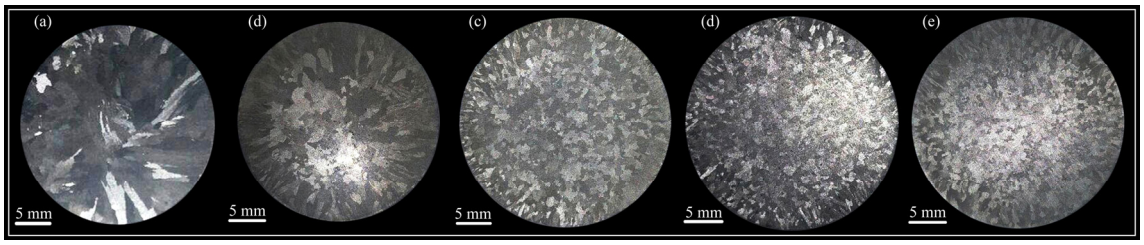

Fig. 6 Grain structures of base (a), C0.5 (b), C1 (c), C2 (d), and C3 (e) alloys

the base alloy to the equiaxed structures in which the effective grain size has decreased by about 60%. The variation of average grain size against Cu content is illustrated in Fig. 7. The refining effect of Cu can be explained by the occurrence of constitutional undercooling [23] as a result of solute rejection in front of the solid liquid interface.

Table 3 shows the effect of Cu on the tensile properties and quality index of A356 alloy. It is perceived from Table 2 that with increasing the Cu content from 1% in the base alloy to about 3% in C3 alloy, the tensile strength increases by almost 30%, reaches up to 248 MPa at 1.5% Cu, and then decreases by further addition of Cu up to 3%. Although, the elongation decreases continuously by about 40% as Cu increases from 1% in the base alloy up to about 3% in C3 alloy.

The positive effect of Cu (<1.5%) on the tensile strength can be attributed to its solid solution strengthening and the dispersion hardening of hard Cu-containing intermetallics [8,24]. The negative effect of Cu (>1.5%) on the tensile strength, however, seems to be due to the high fractions of brittle θ-Al_2Cu particles at grain boundaries (Figs. 3(b−d)). The effect of θ-Al_2Cu compounds on the tensile properties can be also verified from the fractured surfaces of tensile specimens, as shown in Fig. 8.

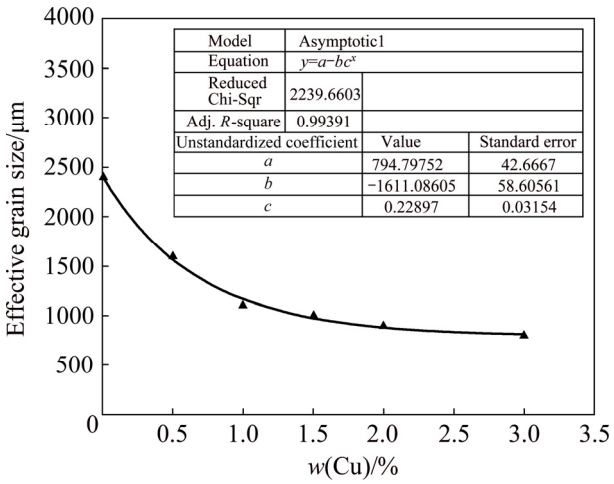

Fig. 7 Effect of Cu content on effective grain size

Table 3 Effect of Cu content on tensile properties and quality index of A356 alloy

Alloy	UTS/MPa	Elongation/%	Q_i
Base	189.1±9.2	9.2±0.3	333.7
C0.5	199.7±8.1	8.2±0.2	336.2
C1	232.4±6.2	7.8±0.5	365.7
C1.5	247.9±8.7	6.4±0.5	368.2
C2	242.9±6.1	5.9±0.4	358.0
C3	211.5±9.9	5.5±0.6	321.8

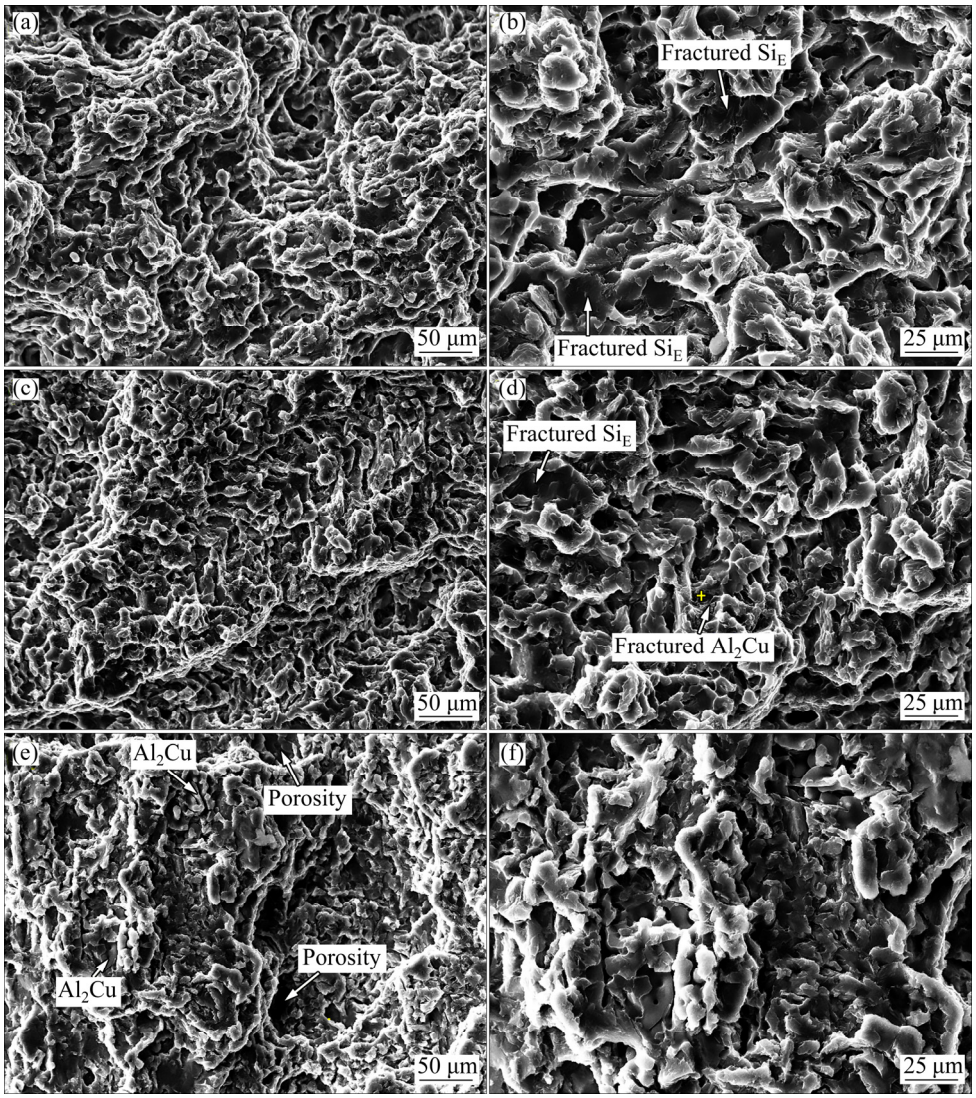

Fig. 8 SEM images of fracture surfaces of selected alloys at different magnifications: (a, b) Base alloy; (c, d) C1.5 alloy; (e, f) C3 alloy

Figures 8(a, b) show the morphology of the fracture surface of the base alloy at two different magnifications. The presence of fractured Si particles on the surface is quite evident and implies their key role in the transgranular fracture of this alloy (Fig. 8(a)). Figures 8(c, d) represent the fracture surface of 1.5Cu sample. In agreement with the tensile properties results (Table 3), the presence of few dimples along with the cleavage patterns related to the Si_E and Al_2Cu particles resembles a quasi-cleavage fracture on this sample. The fracture surface of 3.0Cu sample at different magnifications is depicted in Figs. 8(e, f). The significant amounts of fractured Al_2Cu and Si_E particles are quite evident, implying their contribution to the premature fracture of the sample.

The negative effect of Cu on the elongation of A356 alloy might be also explained by the increase in the fraction of brittle Cu-bearing intermetallics and the fraction of microporosities. The effect of Cu on the volume fraction of microporosities in A356 alloy is illustrated in Fig. 9. As can be seen, the addition of 3% Cu increases the volume fraction of micropores by more than 120% from 0.8% in the base alloy to about 1.8% in C3 alloy. The formation of Cu-induced microporosities, which is also quite evident on the fracture surface of C3 sample, is attributed to the progressive segregation of the Cu atoms in front of the solid−liquid interface which increases the activity coefficient of hydrogen, thereby decreases the hydrogen solubility and gives rise to the higher volumetric shrinkage [8,11,12].

The quality index (Q_i) approach is also applied to investigating the effect of different Cu contents on the quality of A356 alloy. The quality index value (Q_i), defined by Eq. (4), combines the tensile strength (R_m) and the ductility (δ), and is a much better indicator of the true tensile properties of the alloys rather than either

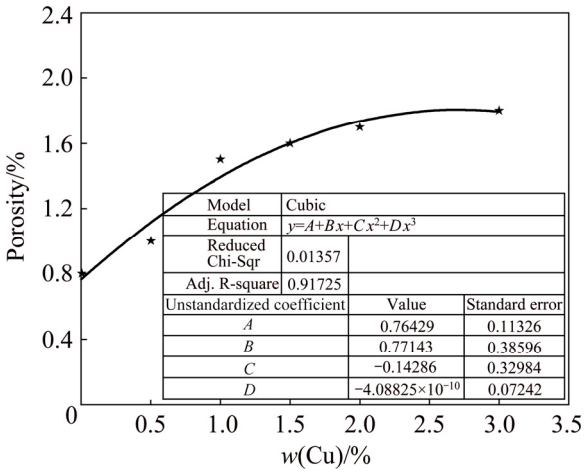

Fig. 9 Effect of Cu content on volume fraction of microporosities

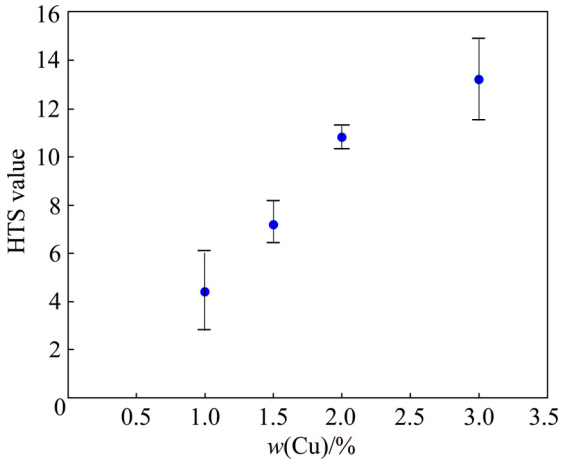

Fig. 10 Variation of HTS with Cu content

tensile strength or elongation alone:

$$Q_i=R_m+k\lg\delta \quad (4)$$

where k is 150 MPa for A356 alloy [25,26].

The effect of Cu on the Q_i is illustrated in Table 3. As seen, the Q_i follows much the same trend as tensile strength with respect to the Cu content. It increases by Cu content, reaches a maximum value of (253±14) MPa at about 1.5% Cu, and then decreases by further addition of Cu up to 3%.

3.2 Effect of Cu on hot tearing susceptibility of A356 alloy

The effect of Cu on the hot tearing susceptibility (HTS) of A356 alloy is shown in Fig. 10. As can be seen, the addition of Cu up to 0.5% has negligible effect, if any, on the HTS value. Further addition of Cu up to 3.0%, however, increases the HTS by almost 33%. The negative effect of Cu on the HTS of A356 alloy is also evident from the footprint charts, as shown in Fig. 11, where the area of the charts increases by the increase of Cu content and severer hot tears are seen on the shorter rods (C-rod) that are naturally more resistant to the hot tearing.

Despite the fact that Cu improves the high-temperature strength and thermal stability and decreases the coefficient of thermal expansion (CTE) of A356 alloy [4,9,10], its addition (>1.0%) increases hot tearing susceptibility. The grain refinement (Fig. 7) and the morphology change from columnar-equiaxed in the base alloy to fully equiaxed in the Cu-containing alloys

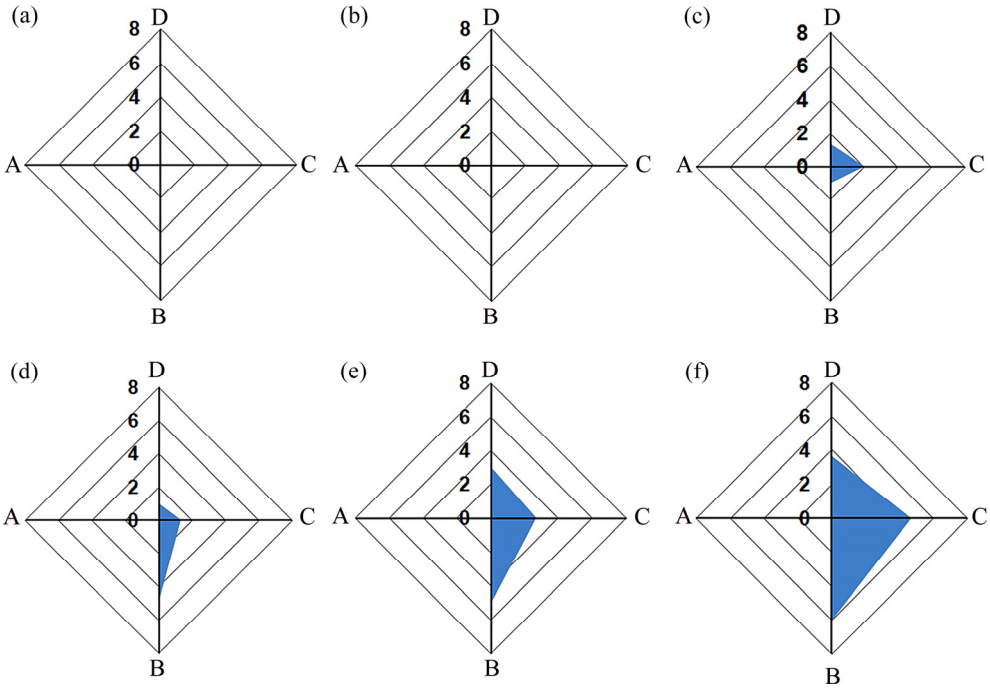

Fig. 11 Footprint charts of base (a), C0.5 (b), C1 (c), C1.5 (d), C2 (e) and C3 (f) alloys

(Fig. 6) can increase the hot tearing resistance probably due to the occurrence of one or more of the following mechanisms:

1) Retarding the dendrites coherency and increasing the time for interdendritic feeding [27];

2) Improving the interdendritic feeding due to the higher capillary pressure between the fine grains [28,29];

3) Delaying the onset of thermal strains [27, 30];

4) Better accommodation of local contraction strains through free movement of the fine grains [31] enveloped by the grain boundaries eutectic liquid.

The effect of Cu on the hot tearing susceptibility of A356 alloy can be also evaluated in terms of its effect on solidification characteristics. Figure 12 shows the variation of the fluidity length of A356 alloy against Cu content. The negative effect of Cu on the fluidity is quite evident where the fluidity continuously decreases by the Cu addition from 2% in the base alloy to about 3% in C3 alloy. To elucidate the origin of fluidity reduction, thermal analysis was performed in order to provide required information about the critical temperatures and the solidification behavior of the alloys.

The cooling curves, the first derivative, and the solid fraction curves of the base and C3 alloys are shown in Fig. 13. As seen, the addition of Cu reduces the solidus temperature, widens the solidification range, and

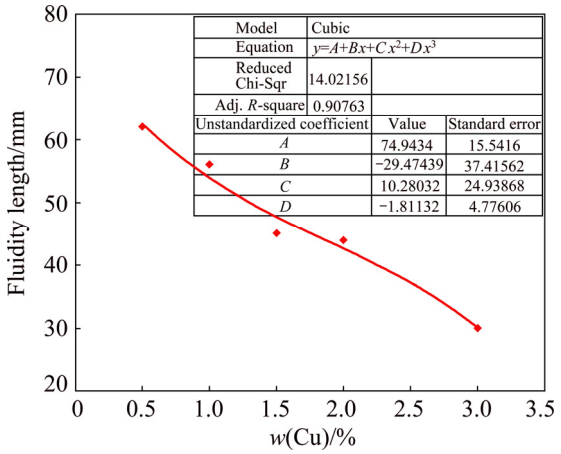

Fig. 12 Effect of Cu content on fluidity length of A356 alloy

changes the solidification type to a mushier state. Under this circumstance, the independent crystallization of the solid nucleus in the liquid alloy can arrest its flow and hence reduces its fluidity. The higher the Cu content, the higher the freezing range of the alloy and, therefore, the lower its fluidity.

The negative effect of Cu on the hot tearing resistance of A356 alloy can be also well described by its effect on widening the freezing range of the alloy. CLYNE and DAVIES [32] and SHABESTARI and

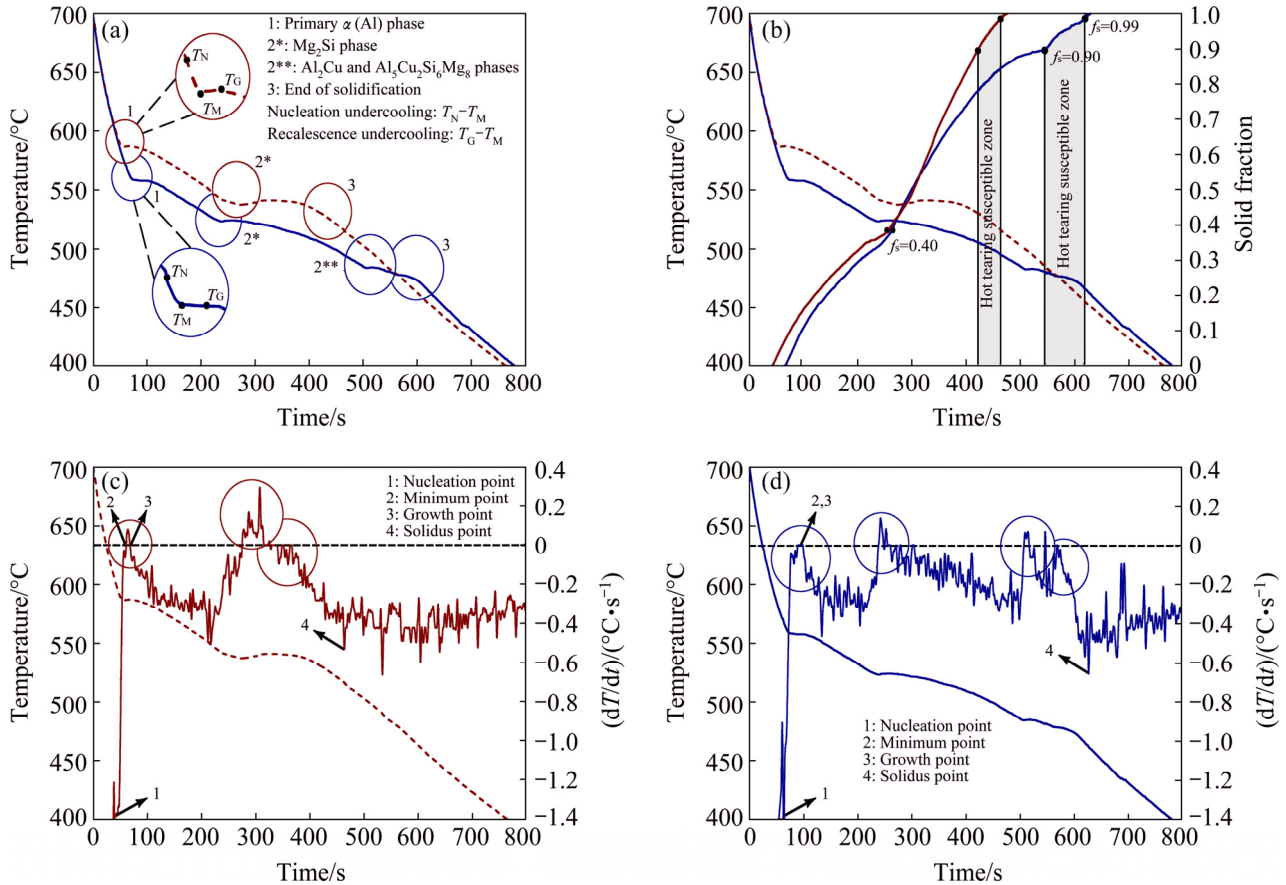

Fig. 13 Cooling curves (a), solid fraction (b), and first derivative curves of base (c) (dashed line) and C3 alloy (d) (solid line)

GHONCHEH [33] proposed the hot cracking sensitivity coefficient (HCSC) (Eq. (5)) to assess the hot tearing susceptibility of alloys. The HCSC is defined as the ratio of the vulnerable time period (t_V), during which hot tears may develop, to the time available for the stress-relief process (t_R), during which mass feeding and liquid feeding occur:

$$\mathrm{HCSC}=\frac{t_V}{t_R}=\frac{t_{0.99}-t_{0.90}}{t_{0.90}-t_{0.40}} \quad (5)$$

where at $t_{0.99}$, $t_{0.90}$, and $t_{0.40}$, the volume fractions of solid (f_s) are 0.99, 0.90, and 0.40, respectively. Thermal analysis results are given in Table 4.

Based on the results presented in Table 4, the addition of 3% Cu enlarges the solidification range and increases the solidification time interval by about 28 °C and 145 min, respectively, as compared to the base alloy. Under this condition, the solidifying alloy spends longer time in the vulnerable state, in which, thin liquid films exist between the solidified dendrites, and there is an increased possibility for hot tear cracks to develop, once the required stress level is reached. The fluidity reduction also reduces the feeding ability of interdendritic liquid during the final stages of solidification, thereby encourages the formation of shrinkage porosities and decreases the healing chance of already-developed hot tear cracks.

Figure 14 illustrates the hot tear surfaces of selected experimental alloys. Dendritic morphology and the occurrence of interdendritic/intergranular fracture are quite evident on the fracture surfaces. The primary α(Al) dendrites covered by Cu-rich eutectic liquid indicate that hot tear cracks are most probably originated through interdendritic separation.

The fracture surface of C1 alloy is smooth and bumpy with little evidence of intergranular tears (Figs. 14(a, b)). In accordance to its low HTS value (Fig. 10), the bumpy appearance of the surface demonstrates that interdendritic liquid has been present at the initiation of hot tearing before dendrite arms being coalescence with neighbors. The smooth appearance of the fracture surface and the fewer occurrences of intergranular tears also confirm that sufficient amounts of eutectic liquid flowing within dendrites channels percolate into the interdendritic voids and cracks and heal them in a process referred to as “self-healing” (Fig. 15). Moreover, in the presence of more eutectic liquid, it is more likely that the solidifying alloy can tolerate the rising tension.

Figures 14(c, d) reveal the hot tear fracture surface of C1.5 alloy. The dendritic morphology and the formation of liquid folding over the primary dendrites reveal the vain attempt of the eutectic liquid to heal the tears. With increasing the Cu content of the alloy, the increased concentration of low-melting-point segregates in interdendritic regions promotes the mushy solidification, increases the permanence of a liquid layer among the dendrites, and gives rise to the higher hot tearing susceptibility. The morphologies of hot tear surface in C3 alloy are depicted in Figs. 14(e−g). The rough dendritic nature of the fracture surface and the occurrence of severe interdendritic and/or intergranular microcracks indicate that interdendritic separation has occurred in the presence of a liquid film, but the volume and/or fluidity of the liquid has not been probably high enough to be able to properly cover the surface of dendrites or heal the hot tear microcracks. This behavior is attributed to the wide freezing range of the alloy which increases the time, during which the alloy is vulnerable to hot tearing, decreases the feeding ability of interdendritic liquid, and promotes the formation of micro-shrinkage cavities that further decreases the alloy strength, which in turn reduces the cross-sectional area.

Table 4 Thermal analysis data of base and C3 alloys

Alloy	Nucleation temperature, T_N/°C	Minimum temperature, T_{Min}/°C	Growth temperature, T_G/°C	Solidus temperature, T_S/°C	Nucleation undercooling, ΔT_N/°C	Recalescence undercooling, ΔT_R/°C
Base	595.8	586.7	587.1	515.9	9.1	0.4
C3	569.4	557.7	557.7	461.5	11.7	0

Alloy	Nucleation time, t_N/s	Solidus time, t_S/s	Solidification temperature interval, ΔT/°C	Solidification time interval, Δt/s	Hot cracking sensitivity coefficient, HCSC
Base	44.8	463.4	79.9	418.6	0.25
C3	62.2	626.4	107.9	564.2	0.27

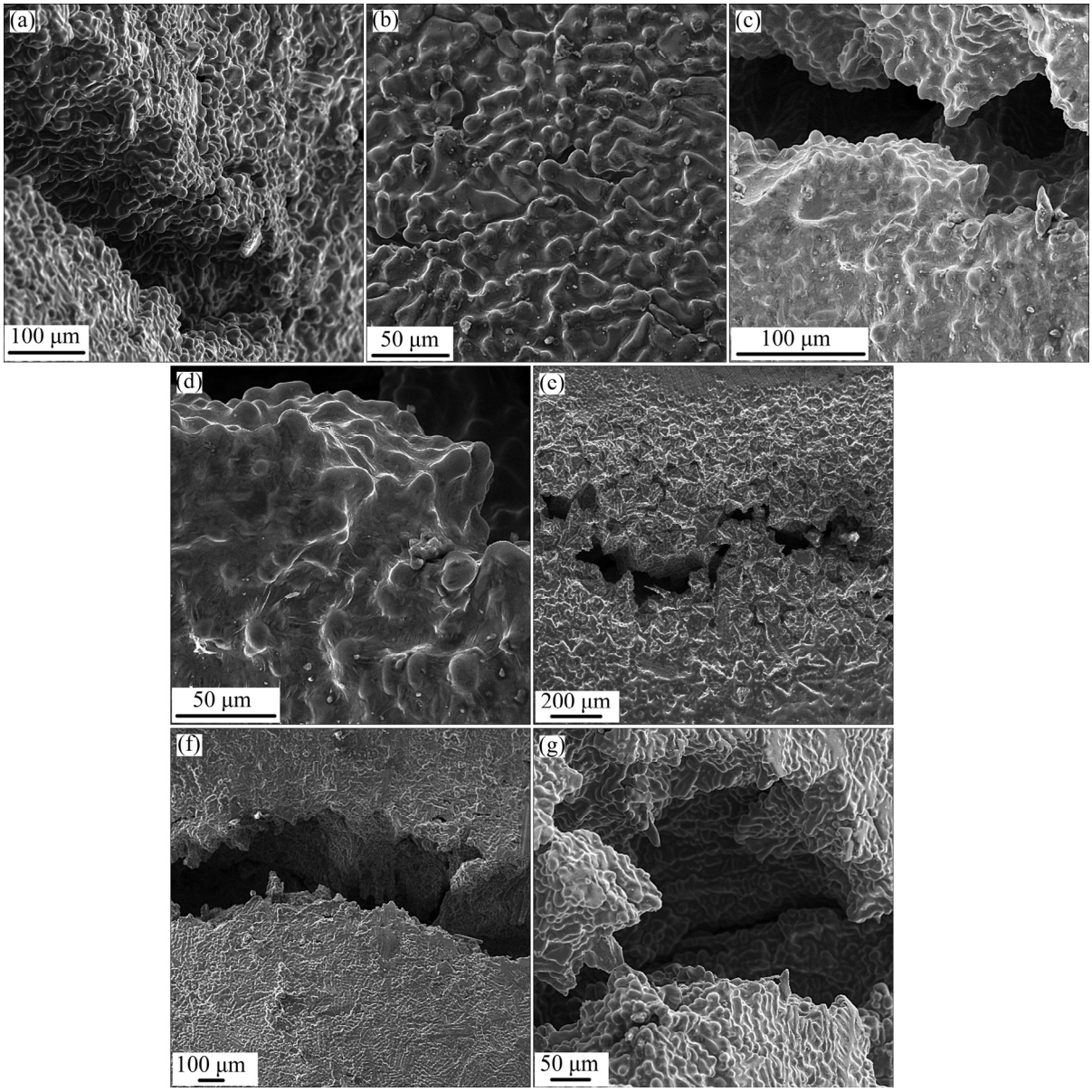

Fig. 14 SEM images of hot tear fracture surfaces: (a, b) C1 alloy; (c, d) C1.5 alloy; (e, f, g) C3 alloy

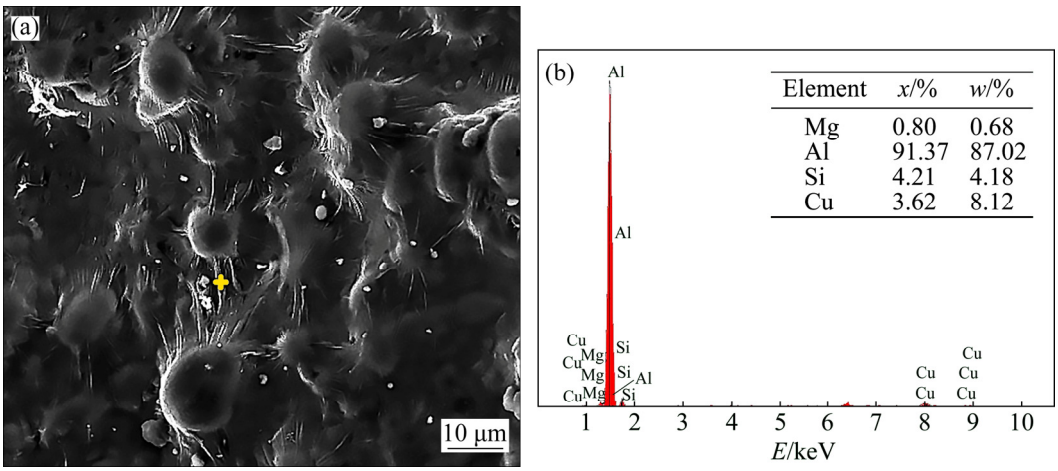

Fig. 15 SEM image (a) and EDS analysis (b) of liquid folds formed on dendrite bumps in C1 alloy

4 Conclusions

1) The microstructure of A356 alloy mainly consists of primary α(Al), eutectic Si, and Mg_2Si intermetallic. Cu addition intensifies the precipitation of θ-Al_2Cu phase as two distinct forms of blocky and ternary eutectic Al−Al_2Cu−Si_E pocket, and quaternary AlMgCuSi phase. Furthermore, Cu addition facilitates the transition from columnar-equiaxed to full-equiaxed structure associated with refining the effective grain size by about 60%.

2) With increasing the amount of Cu from 1% in the base alloy to 3% in C3 sample, the tensile strength reaches up to its maximum value of 248 MPa at 1.5% Cu and after that goes downward, while the elongation continuously decreases by about 40% in C3 sample compared with base alloy. Also, the quality index of samples follows the twofold trend as similar as the trend explained about tensile strength.

3) Predominant mechanism in increasing the tensile strength by adding Cu up to 1.5% is ascribed to solid solution strengthening caused by hard Cu-rich compounds, whilst the detrimental effect of 2% and 3% Cu on tensile strength can be related to high volume fraction of brittle Al_2Cu particles at grain boundaries. In addition, continuous drop in elongation by Cu addition might be also described by the increase in the fraction of brittle Cu-bearing intermetallics as well as the volume fraction of microporosities from 0.8% in the base alloy to approximately 1.8% in C3 sample.

4) The hot tearing sensitivity is intensified about 33% by increasing Cu content to 3% due to suppressing the fluidity of A356 alloy. Higher Cu content widens the freezing range in which the solidifying alloy is exposed to broaden mushy-state interval, and independent crystallization of the solid nucleus in the adjacent liquid can arrest percolation of the molten metal into interdendritic regions. From thermal analysis aspect of view, higher amounts of Cu enlarge the vulnerable zone described by Clyne and Davies criterion in which thin liquid films between the solidified dendrites cannot accommodate stress concentration during solidification contraction at the final stage of mushy zone.

5) In accordance with low hot tearing sensitivity in low-copper alloys, the bumpy appearance of the hot tear surface in C1 sample proves the presence of interdendritic liquid at the initiation of hot tearing before coalescence of dendrite arms to each other. The smooth fracture surface and few intergranular tears also imply that sufficient amounts of eutectic liquid can flow into the interdendritic voids and cracks and heal them in a process called as “self-healing”.

References

[1] WANG Q C. Microstructural effects on the tensile and fracture behavior of aluminum casting alloys A356/A357 [J]. Metallurgical and Materials Transactions A, 2003, 34: 2887−2889.

[2] XU R, ZHENG H, LUO J, DING S, ZHANG S, TIAN X. Role of tensile forces in hot tearing formation of cast Al−Si alloy [J]. Transactions of Nonferrous Metals Society of China, 2014, 24: 2203−2207.

[3] CACERES C H, DAVIDSON C J, GRIFFITHS J R, WANG Q C. The effect of Mg on the microstructure and mechanical behavior of Al−Si−Mg casting alloys [J]. Metallurgical and Materials Transactions A, 1999, 30: 2611−2618.

[4] CACERES C H, SVENSSON I L, TAYLOR J A. Strength-ductility behaviour of Al−Si−Cu−Mg casting alloys in T6 temper [J]. International Journal of Cast Metals Research, 2003, 15: 531−544.

[5] LIU J, KOU S. Crack susceptibility of binary aluminum alloys during solidification [J]. Acta Materialia, 2016, 110: 84−94.

[6] LI S, SADAYAPPAN K, APELIAN D. Characterization of hot tearing in Al cast alloys: Methodology and procedures [J]. International Journal of Cast Metals Research, 2011, 24: 88−95.

[7] SAMUEL E, SAMUEL A M, DOTY H W, VALTIERRA S, SAMUEL F H. Intermetallic phases in Al−Si based cast alloys: New perspective [J]. International Journal of Cast Metals Research, 2014, 27: 107−114.

[8] SHABESTARI S G, MOMENI H. Effect of copper and solidification conditions on the microstructure and mechanical properties of Al−Si−Mg alloys [J]. Journal of Materials Processing Technology, 2004, 153−154: 193−198.

[9] SALLEH M S, OMAR M Z. Influence of Cu content on microstructure and mechanical properties of thixoformed Al−Si−Cu−Mg alloys [J]. Transactions of Nonferrous Metals Society of China, 2015, 25: 3523−3538.

[10] VANEETVELD G, RASSILI A, PIERRET J C, LECOMTE-BECKERS J. Conception of tooling adapted to thixoforging of high solid fraction hot-crack-sensitive aluminium alloys [J]. Transactions of Nonferrous Metals Society of China, 2010, 20: 1712−1718.

[11] CACERES C H, DJURDJEVIC M B, STOCKWELL T J, SOKOLOWSKI J H. The effect Cu content on the level of microporosity in Al−Si−Cu−Mg casting alloys [J]. Scripta Materialia, 1999, 40: 631−637.

[12] EDWARDS G A, SIGWORTH G K, CACERES C H, STJOHN D H, BARRESI J. Microporosity formation in Al−Si−Cu−Mg casting alloys [J]. AFS Transactions, 1997, 105: 809−818.

[13] LIN S, ALIRACI C, PEKGULERYUZ M O. Hot-tear susceptibility of aluminum wrought alloys and the effect of grain refining [J]. Metallurgical and Materials Transactions A, 2007, 38: 1056−1068.

[14] KAMGA H K, LAROUCHE D, BOURNANE M, RAHEM A. Solidification of aluminum-copper B206 alloys with iron and silicon additions [J]. Metallurgical and Materials Transactions A, 2010, 41: 2844−2855.

[15] LI Y, BAI Q L, LIU J C, LI H X, DU Q, ZHANG J S, ZHUANG L Z. The influences of grain size and morphology on the hot tearing susceptibility, contraction, and load behaviors of AA7050 alloy inoculated with Al−5Ti−1B master alloy [J]. Metallurgical and Materials Transactions A, 2016, 47: 4024−4037.

[16] LI S, SADAYAPPAN K, APELIAN D. Effects of mold temperature and pouring temperature on the hot tearing of cast Al−Cu alloys [J]. Metallurgical and Materials Transactions B, 2016, 47: 2979−2990.

[17] OYA S, FUJII T, OHTAKI M, BABA S. Solidified structure and hot tearing of Al−4.5%Cu and Al−4.5%Cu−5%Si alloys containing various additives [J]. Journal of Japan Institute of Light Metals, 1983,

34: 511−516.
[18] LI M, WANG H, WEI Z, ZHU Z. The effect of Y on the hot-tearing resistance of Al−5wt.%Cu based alloy [J]. Materials and Design, 2010, 31: 2483−2487.
[19] NAGAUMI H, SUZUKI S, OKANE T, UMEDA T. Effect of iron content on hot tearing of high-strength Al−Mg−Si alloy [J]. Materials Transactions, 2006, 47: 2821−2827.
[20] SWEET L, TAYLOR J A, COUPER M J, EASTON M. Hot tearing in Al−Mg−Si alloys with minor additions of Cu or Mn [J]. Materials Science Forum, 2011, 693: 217−223.
[21] BIRRU A K, BENNY KARUNAKAR D. Effects of grain refinement and residual elements on hot tearing of A713 aluminium cast alloy [J]. Transactions of Nonferrous Metals Society of China, 2016, 26: 1783−1790.
[22] PEKGULERYUZ M O, LIN S, OZBAKIR E, TEMUR D, ALIRAVCI C. Hot tear susceptibility of aluminium–silicon binary alloys [J]. International Journal of Cast Metals Research, 2010, 23: 310−320.
[23] DAVIS S H. Theory of solidification [M]. Cambridge, UK: Cambridge University Press, 2001.
[24] ZEREN M, KARAKULAK E, GUMUS S. Influence of Cu addition on microstructure and hardness of near-eutectic Al−Si−*x*Cu alloys [J]. Transactions of Nonferrous Metals Society of China, 2011, 21: 1698−1702.
[25] ALEXOPOULOS N D, PANTELAKIS S G. Quality assessment of artificially aged A357 aluminum alloy cast ingots by introducing approximate expressions of the quality index Q_D [J]. Metallurgical and Materials Transactions A, 2004, 35: 3079−3089.
[26] AMMAR H R, SAMUEL A M, SAMUEL F H, SIMIELLI E, SIGWORTH G K, LIN J C. Influence of aging parameters on the tensile properties and quality index of Al−9 Pct Si−1.8 Pct Cu−0.5 Pct Mg 354-type casting alloys [J]. Metallurgical and Materials Transactions A, 2012, 43: 61−73.
[27] EASTON M A, WANG H, GRANDFIELD J, STJOHN D H. An analysis of the effect of grain refinement on the hot tearing of aluminium alloys [J]. Materials Science Forum, 2004, 28: 224−229.
[28] EASTON M A, STJOHN D H, SWEET E. Grain refinement and hot tearing of aluminium alloys—How to optimise and minimize [J]. Materials Science Forum, 2010, 630: 213−221.
[29] SUBROTO T, MIROUX A, BOUFFIER L, JOSSEROND C, SALVO L, ESKIN D G, KATGERMAN L. Formation of hot tear under controlled solidification conditions [J]. Metallurgical and Materials Transactions A, 2014, 45: 2855−2862.
[30] RATHI S K, SHARMA A, DI SABATINO M. Effect of mould temperature, grain refinement and modification on hot tearing test in Al−7Si−3Cu [J]. Engineering Failure Analysis, 2017, 79: 592−605.
[31] MI G, LIU X, ZHU Z, WANG H, Effects of chill casting processes on secondary dendrite arm spacing and densification of Al−Si−Mg alloy [J]. Transactions of Nonferrous Metals Society of China, 2007, 17: 1012−1017.
[32] CLYNE T W, DAVIES G J. Influence of the composition on solidification cracking susceptibility in binary alloy system [J]. British Foundryman, 1981, 74: 65−73.
[33] SHABESTARI S G, GHONCHEH M H. Investigation on the effect of cooling rate on hot tearing susceptibility of Al2024 alloy using thermal analysis [J]. Metallurgical and Materials Transactions B, 2015, 46: 2438−2448.

Al−7Si−0.35Mg−*x*Cu 合金的品质系数和热裂敏感性

R. TAGHIABADI[1], A. FAYEGH[1], A. PAKBIN[1], M. NAZARI[1], M. H. GHONCHEH[2]

1. Department of Materials Science and Ceramic Engineering, Imam Khomeini International University, Qazvin, Iran;
2. School of Metallurgy and Materials Engineering, Iran University of Science and Technology, Tehran, Iran

摘　要：研究铜添加量(0.5%、1%、1.5%、2%、3%，质量分数)对 A356 合金的品质系数(Q_i)和热裂敏感性(HTS)的影响。结果显示，当铜添加量达到 1.5%时，Q_i 增加了约 10%，这可能是由于富铜的 Al_2Cu 相和 AlMgCuSi 化合物的固溶强化和弥散硬化。然而，继续提高 Cu 添加量到 3%，Q_i 反而降低了近 12%，这很可能是因为显微组织中脆性富 Cu 金属间化合物和微孔体积的增加导致抗拉强度和伸长率降低。用约束杆铸造法测试 A356 合金的热裂敏感性，结果显示随着铜含量的增加，其 HTS 也增加。热分析结果表明，铜拓宽了合金的凝固范围，进而降低了其流动性，增加了糊状合金暴露在热裂易感区的时间。高铜合金热裂表面的 SEM 也表明，其表面粗糙，且存在枝晶间/晶粒间微裂纹，这也证明了在凝固后期，合金萌生了热裂，没有足够的裂纹修复时间。

关键词：Al−Si−Mg 合金；热裂；品质系数；铜；流动性

(Edited by Xiang-qun LI)